First-principles calculations of the diffusion of atomic oxygen in nickel: thermal expansion contribution

2007 J. Phys.: Condens. Matter 19 296201

(http://iopscience.iop.org/0953-8984/19/29/296201)

IOP PUBLISHING JOURNAL OF PHYSICS: CONDENSED MATTER

J. Phys.: Condens. Matter **19** (2007) 296201 (8pp) doi:10.1088/0953-8984/19/29/296201

First-principles calculations of the diffusion of atomic oxygen in nickel: thermal expansion contribution

E H Megchiche[1,2], M Amarouche[2] and C Mijoule[3]

[1] Laboratoire de Physique Quantique, IRSAMC (UMR 5626), Université Paul Sabatier, 118 route de Narbonne, 31062, Toulouse Cedex 4, France
[2] Laboratoire de Physique et Chimie Quantique (LPCQ), Université Mouloud Mammeri, Tizi-Ouzou, Algeria
[3] CIRIMAT UMR CNRS/INP/UPS, Ecole Nationale d'Ingénieurs en Arts Chimiques et Technologiques (ENSIACET), 118 Route de Narbonne, F-31077 Toulouse cedex, France

E-mail: Claude.Mijoule@ensiacet.fr

Received 20 March 2007, in final form 5 May 2007
Published 5 July 2007
Online at stacks.iop.org/JPhysCM/19/296201

Abstract

Within the framework of density functional theory using the projector augmented-wave (PAW) method, we present some energetic properties of atomic oxygen interstitials in crystalline Ni, i.e. the insertion and activation energies of the O diffusion. Concerning the activation energy, two pathways for the migration process are studied. The charge transfer process between atomic oxygen and nickel atoms is analysed in the interstitial sites. We find that the interstitial octahedral site (O site) is lower in energy than the tetrahedral site (T site). The most favourable pathway for the migration between two octahedral sites corresponds to an intermediate metastable state located in a tetrahedral site. Concerning the charge transfers we find that the atomic oxygen ionizes as O^- and that the electron migrates essentially from the Ni nearest neighbours of atomic oxygen. In addition, the thermal expansion contribution through the dilatation of the solid is studied. When the thermal expansion is introduced, we show that the insertion process is stabilized and that the tetrahedral insertion energy becomes nearly equal to the octahedral ones. However, the activation energy decreases with the dilatation. Taking into account the thermal expansion effects, our results are consistent with the more reliable experimental data.

1. Introduction

Nickel and nickel-based alloys are vitally important to modern industry because of their ability to withstand a wide variety of severe operating conditions involving corrosive environments, high temperatures, high stresses, and combination of these factors. The solubility and diffusivity of oxygen plays an important role in the kinetics of the process of internal oxidation of nickel alloys, i.e. the increase of the creep resistance. Furthermore, dissolved oxygen may

greatly affect the mechanical properties of the metal [1]. The solubility and diffusion of atomic oxygen in nickel has led to several reports in the literature. The solubility of oxygen in nickel was first reported by Seybolt *et al* [2]. Thirteen years later Alcock and Brown [3] and Goto and Nokami [4] obtained the solubility of oxygen in nickel by a thermogravimetric method. They also estimated the oxygen diffusivity in nickel. These authors [2–4] indicated a decrease of the solubility with increasing temperature, in contrast to most metal–oxygen systems like silver–oxygen [5]. Therefore, doubts can be expressed about these results. From the solubility data of Seybolt [2] for pure nickel, some authors derived the diffusivity of oxygen in nickel. By internal oxidation investigation, Goto and Nomaki [4], Barlow and Grundy [6] and Lloyd and Martin [7] deduced activation energies of 3.13, 3.23 and 4.29 eV respectively in the temperature range 900–1350 °C. Zholobov and Malev [8] derived oxygen diffusivity values for temperatures below 850 °C and thus determined the activation energy for the diffusion of oxygen in nickel. Kerr [9] obtained the activation energy by using an electrolytic cell in a coulometric titration technique. However, there is a spread of a factor two in the activation energy among the reported experimental investigations (from 1.88 to 4.29 eV). Several years later, Park and Altstetter [10] determined the diffusivity and thermodynamic functions of oxygen dissolved in solid nickel. Their results concerning the activation energy were obtained by two different methods, i.e. potentiometric (1.70 eV) and potentiostatic (0.94 eV), and they obtained a solubility energy of 0.57 ± 0.01 eV. Their data differ significantly from those in previous reports. They point out that the advantage of their electrochemical technique is that no quenching is involved and no chemical analysis is required, in contrast with the previous experimental studies. Consequently, their study seems to be the most reliable because, on the one hand, it is carried out without any intermediate value of the solubility energy, and on the other hand, it is done on a pure nickel substrate.

To our knowledge, no theoretical investigations of the diffusion of oxygen in solid nickel are available. Nevertheless two recent theoretical works used first-principles calculations to study the diffusion process (i.e. the determination of the solubility and activation energies) of light atoms in metals. Crocombette *et al* [11] studied the insertion of oxygen atoms in silver and their interactions with vacancies in the framework of the density functional theory (DFT). Solution energies of O in Ag were thus determined for various insertion sites. Siegel and Hamilton [12] investigated the solubility, diffusion and clustering of carbon in nickel. These two theoretical studies used the same kind of theoretical approach (DFT).

In this work, we are concerned with the diffusion process of atomic oxygen in nickel. The insertion energy of oxygen is calculated with the DFT approach for octahedral and tetrahedral interstitial sites. Furthermore, the activation energies are determined by considering two possible pathways for the migration of O. In order to compare our results with experimental data, the effects of thermal expansion on various energies are examined.

2. Methods of calculation

The calculations are performed within the DFT formalism and the pseudo-potential approximation. They are done by means of the Vienna *ab initio* simulation program (VASP) developed at the Institut für Materialphysik of the Universität Wien [13, 14]. The spin-polarized self-consistent Kohn–Sham equations are solved within the projected-augmented wave (PAW) method [15, 16]. This leads to a powerful efficiency concerning the computation time. The generalized gradient approximation (GGA) is used with the exchange–correlation functional of Perdew and Wang (PW91) [17]. The GGA approach is chosen because some recent theoretical studies showed that it is more adapted than other approximations like the local density approximation to describe various properties of Ni bulk [18–20] or to calculate the

formation and migration enthalpies of vacancies in nickel [20]. Concerning the computational parameters, the plane-wave energy cut-off is fixed to 14.7 Ryd (400 eV) for all calculations, independently of the size of the unit cell. On the other hand, $4 \times 4 \times 4$ and $6 \times 6 \times 6$ Monkhorst–Pack [21] meshes are used to sample the Brillouin zone in the reciprocal space, depending on the size of the studied unit cell. Concerning the energy of the isolated oxygen atom, we introduced the spin polarization effects in order to describe the triplet nature of its ground state. To determine the insertion energies of oxygen, two sizes of face-centred cubic (fcc) primitive cell were tested, i.e. 32 and 108 lattice sites per unit cell. By periodicity, the first one leads to an oxygen–oxygen distance of 7.04 Å while the second one gives 10.56 Å. In each energetic calculation (insertion and diffusion) we take into account the lattice relaxation. The relaxation is introduced by using a conjugate-gradient algorithm for insertion energies and all ions are allowed to relax while the supercell volume is kept constant; for the saddle point corresponding to the migration of the atomic oxygen, the energy pathways are obtained by using the nudged elastic band (NEB) method of Henkelman and Jónsson [22, 23]. The charge transfer between oxygen and nickel is determined with the algorithm of Henkelman *et al* [24], which carries out a Bader decomposition [25] of the electronic charge density into atomic contributions. The thermal expansion contribution is estimated by studying the variation of the insertion and activation energies with respect to the lattice parameter a. All energies were calculated for five values of the lattice parameter a.

3. Results and discussion

3.1. Diffusivity and solubility of oxygen in nickel

In order to determine the diffusivity and the solubility of oxygen in nickel, we need to calculate the activation energy $E_{\mathrm{O}}^{\mathrm{act}}$ and the insertion energy $E_{\mathrm{O}}^{\mathrm{ins}}$ of O in Ni. Indeed, the diffusivity is defined as

$$D = D_0 \exp\left(-\frac{E_{\mathrm{O}}^{\mathrm{act}}}{RT}\right) \tag{1}$$

while the solubility is given by

$$C^{\mathrm{s}} = C_0^{\mathrm{s}} \exp\left(-\frac{E_{\mathrm{O}}^{\mathrm{sol}}}{RT}\right) \tag{2}$$

where the solution energy E^{sol} is given by

$$E_{\mathrm{O}}^{\mathrm{sol}} = E_{\mathrm{O}}^{\mathrm{ins}} - \tfrac{1}{2} E_{\mathrm{O}_2} \tag{3}$$

where E_{O_2} is the dissociation energy of the O_2 molecule in the gas phase.

3.1.1. Atomic oxygen insertion and solution energies. Two sites are considered for the insertion of atomic oxygen in nickel: the octahedral (O) and tetrahedral (T) interstitial positions (see figure 1).The insertion energy is defined as

$$E_{\mathrm{O}}^{\mathrm{ins}} = E^{n\mathrm{Ni}} + E_{\mathrm{O}} - E^{n\mathrm{Ni+O}} \tag{4}$$

where $E^{n\mathrm{Ni+O}}$ is the total energy of the supercell containing n Ni atoms and the O atom inserted in the octahedral or tetrahedral site, $E^{n\mathrm{Ni}}$ is the total energy of the supercell, and E_{O} is the energy of the oxygen atom.

Our results are given in table 1. Computations are done with the theoretical lattice parameter calculated by Megchiche *et al* [20]. Concerning the insertion energies we find that the octahedral position is more stable by 0.17 eV, due to a larger geometrical relaxation in the

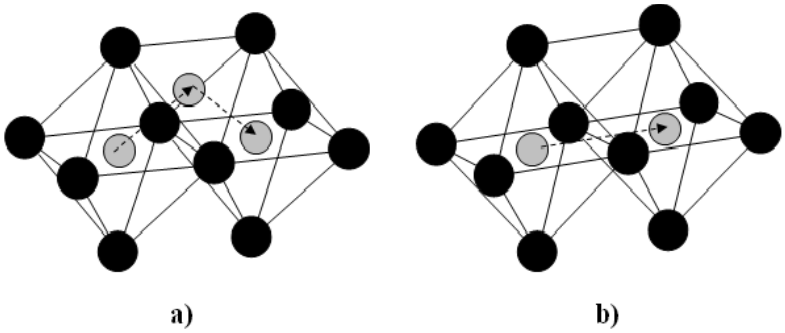

Figure 1. Pathways for the migration of O: (a) O–T–O diffusion pathway; (b) direct O–O diffusion pathway.

Table 1. Insertion energy $E_{\mathrm{O}}^{\mathrm{ins}}$ (in eV), Ni–O nearest neighbour distances $r_{\mathrm{Ni-O}}$ (in Å) and net charges q (in au) of O and nearest-neighbour Ni for the octahedral and tetrahedral interstitial sites.

		Octahedral		Tetrahedral	
		32	108	32	108
Non-relaxed	$E_{\mathrm{O}}^{\mathrm{ins}}$	1.25	1.24	−2.25	−2.28
	$r_{\mathrm{Ni-O}}$	1.76		1.52	
Relaxed	$E_{\mathrm{O}}^{\mathrm{ins}}$	2.65	2.65	2.38	2.48
	$r_{\mathrm{Ni-O}}$	1.92	1.90	1.79	1.78
	q_{Ni}	+0.21		+0.23	
	q_{O}	−1.39		−1.10	
$E_{\mathrm{O}}^{\mathrm{ins}}$ experimental	3.12[a]				

[a] Reference [10].

second case (without relaxation the tetrahedral insertion is unstable). The size of the unit cell has no effect on the octahedral insertion and the change is of 0.1 eV for the tetrahedral one (due to the largest relaxation). Looking at the experimental data obtained by Park and Altstetter [10] (3.12 eV) our most stabilized site (octahedron) has an energy of 2.65 eV which corresponds to an underestimation of 0.47 eV. We can note now that our theoretical results corresponds to a 0 K temperature while the experiments were done in the temperature range of 800–1000 °C. The larger relaxation in the tetrahedral site is confirmed by the largest increase of the Ni–O distance (table 1). We note that the oxygen atom becomes anionic (O^-) when inserted in the bulk and that the electron is migrating essentially from the Ni nearest neighbours; indeed 1.26 electrons migrate from the six nearest-neighbour Ni atoms in the octahedral site (1.26 electrons on O) while 0.92 electrons migrate from the four nearest-neighbour Ni atoms in the tetrahedral site (1.10 electrons on O) (see table 1).

3.1.2. Atomic oxygen diffusion energy. The calculated activation energies for O interstitial diffusion are given in table 2. The migration energies are calculated from the NEB method by using octahedral sites as the end points of the process, and we analyse two different pathways (figure 1). The first NEB calculation (using five images) is the one passing through an adjacent T site via a face of the octahedron (figure 1(a)). The transition state is located near this face slightly in the octahedron. The transition states corresponds to an activation energy of 1.25 eV (see figure 2 and table 2). The second one (the O–O path) is obtained by translating the O

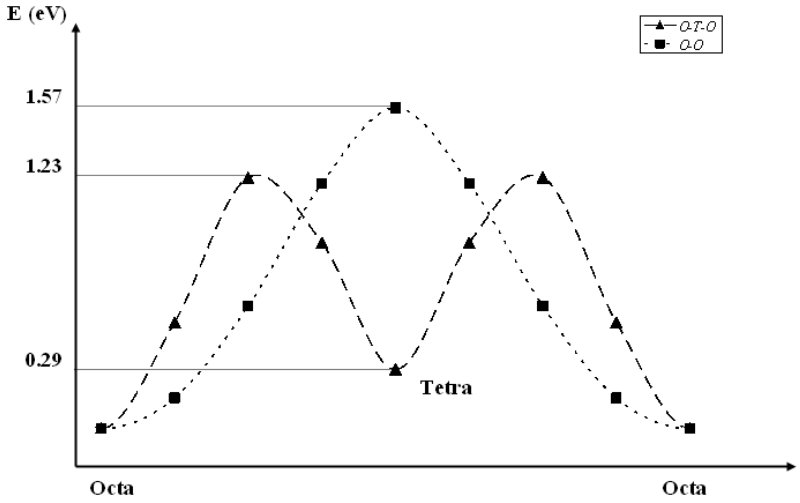

Figure 2. Activation energy of O interstitial diffusion for *O–O* and *O–T–O* pathways by using a 32-atom supercell.

Table 2. Activation energies E_O^{act} (in eV) and Ni–O distances r_{Ni-O} (in Å) at the transition state for both *O–O* and *O–T–O* pathways.

	O–O		*O–T–O*	
	32	108	32	108
E_O^{act}	1.57	1.54	1.23	1.25
r_{Ni-O}	1.66	1.72	1.67	1.74
E_O^{act} experimental	0.94[a], 1.71[b]			

[a] Reference [9]: potentiostatic measurement.
[b] Reference [9]: potentiometric measurement.

atom from one *O* site to the second one, with an intermediate state located in the middle of the edge shared by the two octahedral sites (figure 1(b)). For this path we use also five image points and this leads to an activation energy of 1.54 eV at the saddle point (see figure 2 and table 2). The comparison with experiment is difficult; taking the more recent results of Park and Altstetter [10] they give two estimations with different methods: the potentiometric data gives a diffusion energy of 1.71 eV while the potentiostatic measurements lead to a value of 0.94 eV. Both measurements are obtained in temperature ranges of nearly 800–1400 °C.

3.2. Thermal expansion effects

Dilatation of metals is due to the contribution of anharmonic terms contained in the interaction potential. We study here if both the insertion and activation energies of oxygen in nickel depend or not on the thermal expansion and thus on the temperature. In a recent study of the formation and migration energy of monovacancies in nickel [20] we showed that an accurate interpretation of experimental data needed to take into account the thermal expansion contribution. Two effects contribute to the variation of E_O^{ins} and E_O^{act} when the lattice parameter *a* increases: first a weakening of the nickel–nickel interaction and second a strengthening of the oxygen atom interaction with its Ni nearest neighbours due to a very small relaxation of the lattice around the O inserting site. We present in figure 3 the variation of E_O^{ins} with the

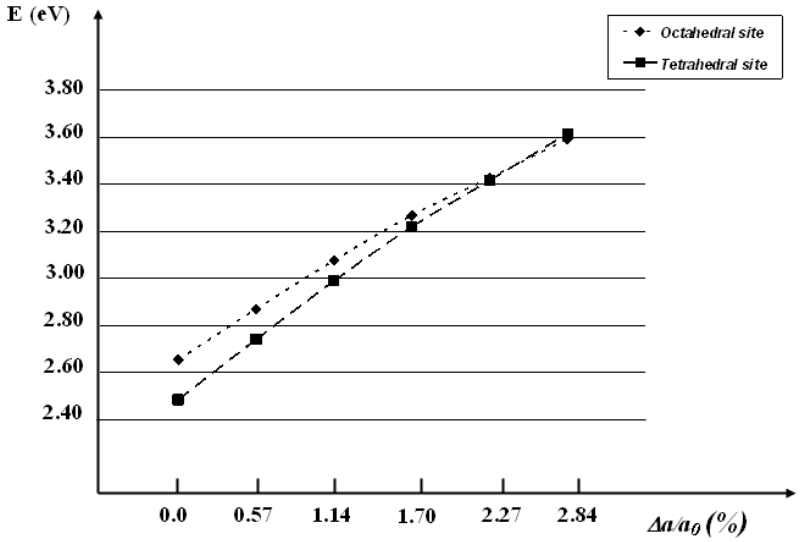

Figure 3. Octahedral and tetrahedral insertion energy variations with the linear thermal expansion.

Table 3. Insertion energy E_O^{ins} (in eV) and Ni–O distances r_{Ni-O} (in Å) of atomic oxygen in nickel for the octahedral and tetrahedral interstitial sites. Results refer to the 108-atom supercell.

	Octahedral		Tetrahedral	
a	E_O^{ins}	r_{Ni-O}	E_O^{ins}	r_{Ni-O}
3.52	2.65	1.90	2.48	1.78
3.56	3.08	1.92	2.99	1.81
3.60	3.43	1.95	3.42	1.82

linear thermal expansion (in per cent) for the tetrahedral and octahedral insertion sites. Our results are obtained with the 108 Ni supercell. Clearly, the insertion becomes more stable when the lattice expands. Furthermore, the stabilization is much more significant for the tetrahedral insertion site for which the relaxation of the lattice is the most important. Both sites become nearly energetically equivalent when the lattice parameter is equal to 3.62 Å. A recent study of Lu *et al* [26] determined the thermal expansion coefficients of nickel numerically in order to obtain a reasonable description of experimental data [27, 28]. In order to correlate the lattice parameter value with the temperature, we used the analytical form proposed by Suh *et al* [28] where the thermal expansion was measured by the dilatation method and by x-ray diffraction. We deduce that the mean temperature at which Park and Altstetter [5] measured the solubility of oxygen ($T = 900\,^{\circ}$C) corresponds to a lattice parameter value of 3.57 Å. By interpolating our results (see figure 3 and table 3) this leads to a calculated E_O^{ins} of 3.16 eV in the octahedral interstitial site, which is in good agreement with the experimental data of Park and Altstetter [5] of 3.12 eV.

Dilatation effects on the activation energies are given in table 4 and visualized in figure 4 for both pathways studied. Clearly, the activation energies decrease significantly with a due to a weakening of the relaxation of the lattice. The O–T–O pathway remains the most stable. Experimental values of 0.94 and 1.71 eV are obtained for mean temperatures of 900 °C and 1125 °C, respectively. They correspond to lattice parameters of 3.57 and 3.59 Å, which lead

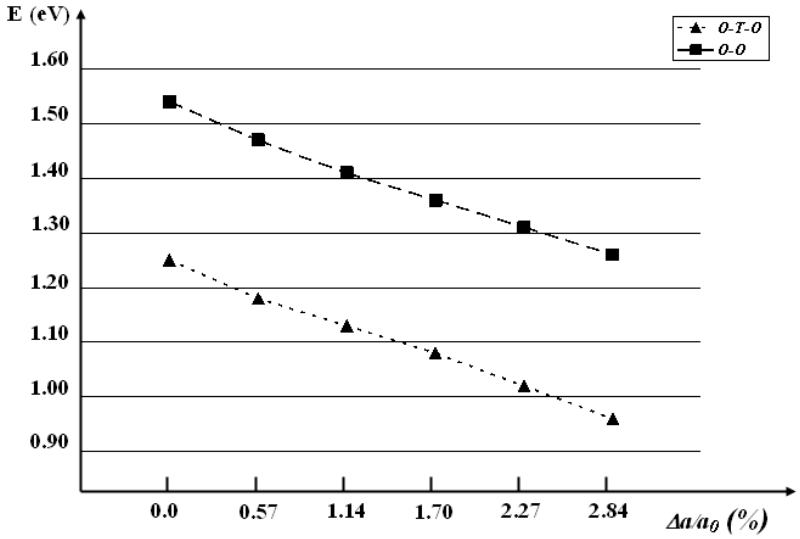

Figure 4. Octahedral–tetrahedral and octahedral–octahedral activation energy variations with the linear thermal expansion a.

Table 4. Activation energies $E_{\mathrm{O}}^{\mathrm{act}}$ (in eV) for some values of the lattice parameter a (in Å).

a	O–O	O–T–O
3.52	1.54	1.25
3.56	1.42	1.13
3.60	1.31	1.02

by interpolation of our results to O–T–O activation energies of 1.10 and 1.05 eV, respectively. Our results are in excellent agreement with the potentiostatic measurement of 0.94 eV.

4. Conclusion

We can conclude briefly the present work, which is the first theoretical determination of the insertion process of atomic oxygen in nickel. We show that, at 0 K, the octahedral insertion site is slightly more stable than the tetrahedral ones. On the other hand, the corresponding calculated insertion energy is significantly underestimated with respect to the most reliable experimental data. Nevertheless, these latter being done at temperatures ranging from 800 to 1200 °C, we studied the dilation effects due to thermal expansion showing that, in this case, our results become more comparable to experimental results. In order to calculate the activation energy, two pathways were studied, showing that the octahedral–octahedral migration of oxygen arises through an intermediate tetrahedral site. As for the insertion, it is shown that with the thermal extension contribution our results compare satisfactorily with experimental data.

Acknowledgments

Computer resources for this job were provided by CALMIP (Toulouse, France) and the computer centre GRID'5000 Nation-Wide Grid Experimental platform funded by the French

Ministry of Research through the ACI GRID Program. We are grateful to Irea Touche (supported by INPT) for gridifying our codes. The calculations were performed using the *ab initio* total-energy program VASP developed at the Institut für Materialphysik of the Universität Wien, Austria.

References

[1] Perusin S, Monceau D and Andrieu E 2005 *J. Electron. Chem. Soc.* **152** E390
[2] Seybolt A U and Fullman R L 1954 *Trans. Metall. Soc. AIME* **200** 548
[3] Alcock C B and Brown P B 1969 *J. Met. Sci.* **3** 116
[4] Goto S, Nomaki K and Koda S 1967 *J. Japan Inst. Met.* **31** 600
[5] Park J-H 1990 *Mater. Lett.* **9** 313
[6] Barlow R and Grundy P J 1969 *Met. Sci. J.* **3** 116
[7] Lloyd G J and Martin J W 1972 *Met. Sci. J.* **6** 7
[8] Zholobov S P and Malev M D 1971 *Zh. Tekh. Fiz.* **41** 677
[9] Kerr R A 1972 *Thesis* The Ohio State University, Columbus; OH, USA
[10] Park J-H and Altstetter C J 1987 *Metall. Trans.* A **18** 43
[11] Crocombette J P, de Monestrol H and Willaime F 2002 *Phys. Rev.* B **66** 024114
[12] Siegel D J and Hamilton J C 2003 *Phys. Rev.* B **68** 094105
[13] Kresse G and Hafner L 1993 *Phys. Rev.* B **47** 558
[14] Kresse G and Furthmuller F 1996 *Phys. Rev.* B **54** 11169
[15] Blochl P E 1994 *Phys. Rev.* B **50** 17953
[16] Kresse G and Joubert D 1999 *Phys. Rev.* B **59** 1758
[17] Perdew J P and Wang Y 1992 *Phys. Rev.* B **46** 12947
[18] Moroni E G, Kresse G, Hafner J and Furthmuller F 1997 *Phys. Rev.* B **56** 15629
[19] Černy M, Pokluda J, Šob M, Friák M and Šandera P 2003 *Phys. Rev.* B **67** 035116
[20] Megchiche E H, Pérusin S, Barthelat J C and Mijoule C 2006 *Phys. Rev.* B **74** 064111
[21] Monkhorst H J and Pack J D 1976 *Phys. Rev.* B **13** 5188
[22] Henkelman G and Jónsson H 1999 *J. Chem. Phys.* **111** 7010
[23] Henkelman G and Jónsson H 2000 *J. Chem. Phys.* **113** 9978
[24] Henkelman G, Arnaldsson A and Jónsson H 2006 *Comput. Mater. Sci.* **36** 354
[25] Bader R 1990 *Atoms in Molecules: A Quantum Theory* (New York: Oxford University Press)
[26] Lu X G, Selleby M and Sundman B 2005 *CALPHAD, Comput. Coupling Phase Diagr. Thermochem.* **29** 68
[27] Yousuf M, Sahu P Ch, Jajoo H K, Rajagopalan S and Govinda Rajan K 1986 *J. Phys. F: Met. Phys.* **16** 373
[28] Suh I K, Ohta H and Waseda Y 1988 *J. Mater. Sci.* **23** 757